# Clear-Water Scour at Pile Groups

Rui Lança[1]; Cristina Fael[2]; Rodrigo Maia[3]; João P. Pêgo[4]; and António H. Cardoso[5]

**Abstract:** Groups of piles are frequently used as bridge foundations. Different group configurations, characterized by different pile spacing, skew-angle, number, and arrangement of pile group columns interact differently with the flow field and lead to different scour patterns and equilibrium scour depth. There have been a number of past studies on the characterization of scouring at pile groups, but most of them report short duration scour experiments. A priori, such short durations may be postulated to inherently carry important uncertainties into existing scour predictors. In this study, 75 long-duration laboratory tests were run under steady, clear-water flow close to the threshold for initiation of sediment motion, to address the effect of time, pile spacing, skew-angle and number of pile group columns on the equilibrium scour depth. Pile groups consisted of matrical arrangements of one, two, or three columns of four rows, with spacings of 1, 2, 3, 4.5, and 6 pile diameters; the tested skew-angles were 0, 15, 30, 45, and 90°. Important contributions were achieved on (1) the impact of the duration of tests on the shape of the scour hole as well as on the precision of coefficients involved in current predictors, (2) the most unfavorable skew angle, (3) the behavior of collapsed pile groups, (4) the maximum scour depth at pile groups composed of a single alignment, and (5) the performance of two current predictors of scour depth at pile groups. Two formulations of a predictor for the calculation of an aggregated pile group factor are suggested. **DOI: 10.1061/(ASCE)HY.1943-7900.0000770.** 

**CE Database subject headings:** Scour; Bridges; Piers; Pile groups.

**Author keywords:** Scour; Bridges; Complex pier; Pile groups; Piers.



## Introduction

For major river crossings, there is increasing use of bridge foundations that consist of a number of piles supporting a pile cap. Piers composed of a column, pile cap, and pile group are known as complex piers. The foundations of the piles are often deep, but if the piles rely on skin friction, rather than end-loading, to support the weight of the bridge, the foundations can be vulnerable to scour.

This study focuses on local scour at pile groups in which the level of the pile cap is above the water level. Pile groups may be composed of one or more columns of piles. Pile groups composed of only one such column of piles are frequently used, without pile cap, to directly support bridge decks. For this reason, this particular group configuration is also referred to as pier alignment herein.

Local scour at pile groups is more complex and difficult to predict than that at single piers. The increased complexity is due to the interaction of vortices generated at individual piles and to the interdependence of scour holes around each pile.

Local scouring at submerged and partly submerged pile groups has already been addressed in the past. However, further research efforts seem to be needed as the number of studies reported in the literature on scouring at pile groups is small. They include those of Hannah (1978), Elliott and Baker (1985), Salim and Jones (1996), Zhao and Sheppard (1999), Smith (1999), Sumer and Fredsøe (2002), Ataie-Ashtiani and Beheshti (2006), and Amini et al. (2012), which mostly report on short-duration scour experiments. Due to this short duration, their results may be postulated to inherently carry uncertainties.

Lança et al. (2012) have shown that clear-water scour depth at pile groups inserted in wide rectangular channels whose bed is composed of uniform non–ripple-forming sand ($D_{50} > 0.6$ mm; $\sigma_D < 1.5$; $D_{50}$ = median sand size; $\sigma_D$ = sand gradation coefficient) is given by (see Fig. 1)

$$\frac{d_{sg}}{D_p} = \varphi\left(\frac{d}{D_p}; \frac{U}{U_c}; \frac{D_p}{D_{50}}; \frac{Ut}{D_p}; \frac{s}{D_p}; \alpha; K_s; m; n\right) \quad (1)$$

where $\varphi$ stands for function; $d_{sg}$ = maximum scour depth at the pile group at instant $t$; $D_p$ = individual pile width; $d$ = approach flow depth; $U$ = approach flow velocity; $U_c$ = approach flow velocity for the threshold of sediment entrainment; $t$ = time; $d/D_p$ = flow shallowness; $U/U_c$ = flow intensity; $D_p/D_{50}$ = sediment coarseness; $Ut/D_p$ = nondimensional time; $s$ = pile spacing; $\alpha$ = pile group skew-angle; $K_s$ = shape factor of individual piles; $m$ = number of rows in the group; $n$ = number of columns in the group; and $s/D_p$ = normalized pile spacing.

Eq. (1) is valid if the approach flow is fully developed and uniform, the flow structure inside the scour hole is free of viscous effects, the wall effects are negligible, and the velocity field is two-dimensional at the central section of the channel (for $B/d > 5$, $B$ = channel width). For sufficiently large values of $d/D_p$, where the scour depth no longer significantly depends on the approach flow depth, Eq. (1) becomes

[1]Departamento de Engenharia Civil, Instituto Superior de Engenharia, Universidade do Algarve, Campus da Penha, 8005-139, Faro, Portugal (corresponding author). E-mail: rlanca@ualg.pt

[2]Departamento de Engenharia Civil e Arquitectura, Faculdade de Engenharia, Universidade da Beira Interior, Calçada Fonte do Lameiro, 6200-358, Covilhã, Portugal. E-mail: cfael@ubi.pt

[3]Departamento de Engenharia Civil, Faculdade de Engenharia, Universidade do Porto, Rua Dr. Roberto Frias, s/n, 4200-465, Porto, Portugal. E-mail: rmaia@fe.up.pt

[4]Departamento de Engenharia Civil, Faculdade de Engenharia, Universidade do Porto, Rua Dr. Roberto Frias, s/n, 4200-465, Porto, Portugal. E-mail: jppego@fe.up.pt

[5]DECivil, Instituto Superior Técnico, Universidade Técnica de Lisboa, Av. Rovisco Pais, 1, 1049-001, Lisbon, Portugal. E-mail: antonio.cardoso@ist.utl.pt

Note. This manuscript was submitted on November 15, 2012; approved on May 2, 2013; published online on May 8, 2013. Discussion period open until March 1, 2014; separate discussions must be submitted for individual papers. This paper is part of the ***Journal of Hydraulic Engineering***, Vol. 139, No. 10, October 1, 2013. © ASCE, ISSN 0733-9429/2013/10-1089-1098/$25.00.

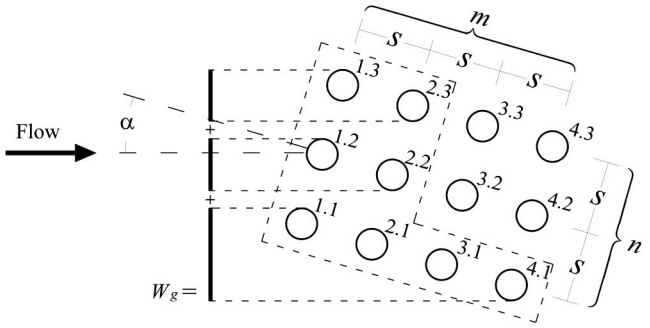


**Fig. 1.** Characteristic variables of a pile group

$$\frac{d_{sg}}{D_p} = \varphi\left(\frac{U}{U_c}; \frac{D_p}{D_{50}}; \frac{Ut}{D_p}; \frac{s}{D_p}; \alpha; m; n\right) \tag{2}$$

if the individual piles are cylindrical ($K_s = 1$). At the equilibrium stage, the maximum scour depth, $d_{sg}$, practically does not depend on time and is denoted here by $d_{sge}$. For $U/U_c = 1$ and $D_p/D_{50} \approx 50$, the equilibrium scour depth is widely recognized to be a maximum. Under these conditions, Eq. (2) becomes

$$\frac{d_{sge}}{D_p} = \varphi\left(\frac{s}{D_p}; \alpha; m; n\right) \tag{3}$$

which may be replaced by

$$K_{pge} = \frac{d_{sge}}{d_{se1}} = \varphi\left(\frac{s}{D_p}; \alpha; m; n\right) \tag{4}$$

In Eq. (4), $d_{se1}$ is the equilibrium scour depth at an isolated pile or pier subjected to the same hydrodynamic conditions as those in Eq. (3), and $K_{pge}$ is an aggregated pile group factor that accounts for spacing, skew angle, the number of columns and the number of rows.

Eq. (4) constitutes the framework for the analysis of the results of the present experimental study as well as of the studies performed to date. Table 1 summarizes the values $\alpha$, $s/D_p$, $n$, $m$, and $U/U_c$ covered by previous studies. It also includes the duration of the reported tests, $t_d$, and describes the shape of the elemental piles cross section.

It is also important to report that, apart from Hannah (1978), Amini et al. (2012) and, in some cases, Ataie-Ashtiani and Beheshti (2006), the remaining authors have used fine sand ($D_{50} < 0.6$ mm), prone to the formation of ripples in the approach flow reach. In the study of Salim and Jones (1996), ripples most likely occurred since $U/U_c \approx 1.0$. Ripples occurrence is an extra source of uncertainty for these results.

Also, according to Simarro et al. (2011), the duration of scour tests should be at least 7 days to allow for the adequate prediction of equilibrium scour at single cylindrical piers. This duration may be short for pile groups since the scouring process can be expected to be more complex and slower. It is clear that, excepting the four tests of Smith (1999), the typical duration of the tests reported in the literature on pile groups is rather short as compared to the time needed to sufficiently approach the equilibrium phase. Consequently, conclusions drawn from the above studies on scouring at pile groups do not seem to guarantee accurate predictions of the equilibrium scour depth.

The present study focus on the effect of pile spacing, $s/D_p$, skew-angle, $\alpha$, as well as number of columns of the pile group, $n$, on the maximum scour depth at pier groups, and pays special attention to the effect of time. The specific question under investigation in this regard is whether the pile group factor defined at a given time, $t$, as $K_{pg} = d_{sg}/d_{s1}$ ($d_{s1}$ = scour depth at a single pile and the same $t$, under the same flow conditions), remains unchanged or not as the scour process evolves through time. For these purposes, a systematic experimental campaign was carried out by performing 75 long-duration ($t_d \geq \approx 7$ days) experiments. These experiments correspond to all the combinations of the following group properties: $n = [1, 2, 3]$, $\alpha = [0°, 15°, 30°, 45°, 90°]$ and $s/D_p = [1, 2, 3, 4.5, 6]$, by keeping $m = 4$.

## Experimental Setup and Procedure

Two flumes were used in the study. One was 28.0 m long, 2.00 m wide, and 1.00 m deep. The maximum flow discharge, measured by an electromagnetic flow meter installed in the hydraulic circuit, was 0.135 $m^3\,s^{-1}$. At the entrance of the flume, two honeycomb diffusers aligned with the flow direction smoothed the flow trajectories and guaranteed a uniform transversal flow distribution. Immediately downstream from the diffusers, a 5.00-m-long bed reach was covered with small gravel to provide proper roughness and guarantee fully developed flow. The central reach of the flume, starting at 14.0 m from the entrance, contained a 3.00-m-long, 2.00-m-wide, and 0.60-m-deep recess box in the bed. At the downstream end of the flume, a tailgate allowed the regulation of the water depth.

The tests were carried out with constant approach flow depth, $d = 0.20$ m, and average velocity, $U = 0.31\ m\,s^{-1} \approx U_c \approx 0.32\ m\,s^{-1}$, as calculated according to Neil (1967).

Individual cylindrical piles were simulated by PVC pipes with diameter $D_p = 50$ mm. Pile groups defined by $m = 4$ were placed at the center of the bed recess box for 60 of the total of

**Table 1.** Control Variables and Nondimensional Parameters of Studies Known to Date

| Study | $\alpha$ (°) | $s/D_p$ | $n$ | $m$ | $U/U_c$ | $t_d$ (h) | Shape[a] |
|---|---|---|---|---|---|---|---|
| Hannah (1978) | 0–90 | 1–21 | 1 | 2 | 0.72 | ≈7 | Circular |
| Elliott and Baker (1985) | 0 | 1.6–13.2 | 1 | 3 | 0.5–1 | NS | RC |
| Salim and Jones (1996) | 0–50 | 1–10 | 3 | 8 | 1.00 | 4 | Square |
| Zhao and Sheppard (1999) | 0–90 | 3 | 3 | 8 | 0.65 | 26 | C + S |
| Smith (1999)[b] | 0–70 | 3; 6 | 2; 3 | 4; 8 | 0.89–0.96 | 65–137 | Square |
| Ataie-Ashtiani and Beheshti (2006) | 0 | 1–11 | 1; 2; 3 | 1; 2; 3 | 0.66–0.88 | ≈8 | Circular |
| Amini et al. (2012)[b] | 0 | 1–6 | 2; 3 | 2; 4; 5 | 0.95 | ≈8 | Circular |

Note: C + S = circular and square; RC = round nose rectangular; NS = not specified.
[a]Shape of the elemental pile cross section.
[b]Only refers to the experiments on uniform spacing and partly submerged pile groups.



J. Hydraul. Eng. 2013.139:1089-1098.

75 different combinations of pile spacing, number of columns, and skew angle. The bed recess box was filled with uniform quartz sand (density, $\rho_s = 2,650\ \text{kg m}^{-3}$; $D_{50} = 0.86$ mm; $\sigma_D = 1.36$).

The second flume was 33.2 m long, 1.00 m wide, and 1.00 m deep; its central reach started at 16.0 m from the entrance; the bed recess box was 3.4 m long, 1.0 m wide, and 0.35 m deep. The maximum flow discharge was $0.090\ \text{m}^3\ \text{s}^{-1}$. The sand used in this flume as well as the imposed flow depth and velocity, diameter of elemental piles, number of rows ($m = 4$) and spacing, $s/D_p = [1, 2, 3, 4.5, 6]$, were the same as in the first flume. Due to width restrictions, this flume was used for only 15 of the total number of tests defined by $\{n = [1],\ \alpha = [0°, 15°]\}$ and $\{n = [2],\ \alpha = [0°]\}$, for $s/D_p = [1, 2, 3, 4.5, 6]$.

Prior to each test, the sand of the corresponding recess box was leveled with the adjacent bed. The area located around the piles was covered with thin metallic plates combined with filter fabric to avoid uncontrolled scour at the beginning of each test. The flumes were filled gradually through independent small-discharge hydraulic circuits, imposing high water depth and low flow velocity. The discharge corresponding to the chosen approach flow velocity was then passed through each flume. Once the discharge and flow depth were established, the metallic plates and filter were carefully removed and the tests started.

Scour was immediately initiated and the depth of scour hole was measured immediately upstream of each elemental pile, to an accuracy of ±1 mm, with adapted point gauges, at high frequency (up to five per hour) during the first day. Afterwards, the interval between measurements increased and, from the first day, three or four measurements were made per day. The minimum duration of each experiment was 7 days. The sand bed approach reach located upstream of the piles stayed undisturbed through the entire duration of the tests.

Five reference experiments for single cylindrical piles defined by $D_p = [50,100,150,200, 400]$ mm were also run for $t_d \approx 7$ days, keeping all the other variables unchanged.

## Results and Discussion

### Data Presentation and Characterization

Table 2 records the characteristic variables and non-dimensional parameters of the 75 experiments. It includes the skew-angle, $\alpha$, the normalized pile spacing, $s/D_p$, the sum of the nonoverlapping elemental pile widths projected on a plane normal to the approach flow direction, $W_g$ (see Fig. 1, in accordance with Richardson and Davis 2001), the channel width, $B$, normalized by $W_g$, test duration, $t_d$, scour depth measured at the end of the test, $d_{sgm}$, and equilibrium scour depth, $d_{sge}$.

For a given group configuration, it may be stated that maxima scour depths are expected since $U/U_c \approx 1.0$ and the bed is composed of uniform non–ripple-forming sand. Although $d/D_p = 4$ and, in accordance with, e.g., Melville and Coleman (2000), the scour depth no longer increases with the flow depth for $d/D_p > 1.43$, this behavior may not have been achieved in this study, particularly for the small values of $s/D_p$, where the group scaling length must be a combination of $D_p$ and $W_g$ instead of $D_p$ alone. Though not characterizing the maxima scour depths for all values of tested $s/D_p$, the results of the study do not lose generality for the chosen values of $s/D_p$, $\alpha$ and $n$ (for $m = 4$ and $s/D_p = 4$).

It may be expected that the ratio $B/d = [5, 10]$ guarantees the absence of wall effects. The ratio $B/W_g$ was at least 5.0, being ≥7.5 in 54 (out of 75) tests and ≥10.0 in 45 tests. Only two tests in the range $7.5 < B/W_g < 10$ corresponded to $s/D_p = 1$ (tests 61 and 66); no test with $5 \le B/W_g < 7.5$ corresponded to values of $s/D_p = 1$, and only four (tests 37, 57, 62 and 67) corresponded to $s/D_p = 2.0$. For values of $s/D_p \ge 3$, the groups are highly permeable and contraction scour may be expected to be dependent on the ratio $B/D_p$, equal to [20, 40], depending on the flume. Referring, e.g., to Ballio et al. (2009), contraction scour may be expected to be negligible with the exception of tests 61 and 66, where the pile group behaved as a unique pile and $B/W_g < 10$.

**Table 2.** Control Variables of the Tests and Equilibrium Scour Depths

| | | $n = 1$ | | | | | | $n = 2$ | | | | | | $n = 3$ | | | | | |
|---|---|---|---|---|---|---|---|---|---|---|---|---|---|---|---|---|---|---|---|
| $\alpha$ (°) | $s/D_p$ | Test | $W_g$ (m) | $B/W_g$ | $t_d$ (day) | $d_{sgm}$ (mm) | $d_{sge}$ (mm) | Test | $W_g$ (m) | $B/W_g$ | $t_d$ (day) | $d_{sgm}$ (mm) | $d_{sge}$ (mm) | Test | $W_g$ (m) | $B/W_g$ | $t_d$ (day) | $d_{sgm}$ (mm) | $d_{sge}$ (mm) |
| 0 | 1.0 | 1 | 0.05 | 20.0 | 11.0 | 138 | 153 | 26 | 0.10 | 10.0 | 13.2 | 239 | 261 | 51 | 0.15 | 13.3 | 8.1 | 286 | 327 |
| | 2.0 | 2 | 0.05 | 20.0 | 16.0 | 146 | 160 | 27 | 0.10 | 10.0 | 15.2 | 185 | 185 | 52 | 0.15 | 13.3 | 7.0 | 206 | 211 |
| | 3.0 | 3 | 0.05 | 20.0 | 13.7 | 144 | 152 | 28 | 0.10 | 10.0 | 14.1 | 174 | 183 | 53 | 0.15 | 13.3 | 7.2 | 178 | 208 |
| | 4.5 | 4 | 0.05 | 20.0 | 16.2 | 167 | 149 | 29 | 0.10 | 10.0 | 9.1 | 140 | 146 | 54 | 0.15 | 13.3 | 8.2 | 153 | 218 |
| | 6.0 | 5 | 0.05 | 20.0 | 11.2 | 135 | 136 | 30 | 0.10 | 10.0 | 7.1 | 143 | 156 | 55 | 0.15 | 13.3 | 8.5 | 141 | 139 |
| 15 | 1.0 | 6 | 0.09 | 11.2 | 11.2 | 147 | 157 | 31 | 0.14 | 14.6 | 7.0 | 226 | 299 | 56 | 0.19 | 10.8 | 8.2 | 284 | 334 |
| | 2.0 | 7 | 0.13 | 7.8 | 13.2 | 157 | 152 | 32 | 0.20 | 9.8 | 7.0 | 198 | 240 | 57 | 0.28 | 7.2 | 8.2 | 240 | 305 |
| | 3.0 | 8 | 0.17 | 6.0 | 15.4 | 159 | 162 | 33 | 0.26 | 7.8 | 7.0 | 181 | 183 | 58 | 0.34 | 5.8 | 7.8 | 211 | 250 |
| | 4.5 | 9 | 0.20 | 5.0 | 8.9 | 173 | 183 | 34 | 0.30 | 6.7 | 7.2 | 174 | 205 | 59 | 0.40 | 5.0 | 8.5 | 178 | 208 |
| | 6.0 | 10 | 0.20 | 5.0 | 11.2 | 164 | 170 | 35 | 0.30 | 6.7 | 8.9 | 179 | 204 | 60 | 0.40 | 5.0 | 7.8 | 158 | 170 |
| 30 | 1.0 | 11 | 0.13 | 16.0 | 6.9 | 204 | 246 | 36 | 0.17 | 11.9 | 6.8 | 225 | 316 | 61 | 0.21 | 9.4 | 7.0 | 272 | 347 |
| | 2.0 | 12 | 0.20 | 10.0 | 6.9 | 204 | 242 | 37 | 0.29 | 7.0 | 6.8 | 245 | 331 | 62 | 0.37 | 5.4 | 8.0 | 264 | 378 |
| | 3.0 | 13 | 0.20 | 10.0 | 7.7 | 183 | 212 | 38 | 0.30 | 6.7 | 7.8 | 216 | 278 | 63 | 0.40 | 5.0 | 8.3 | 249 | 280 |
| | 4.5 | 14 | 0.20 | 10.0 | 7.2 | 147 | 198 | 39 | 0.30 | 6.7 | 6.9 | 185 | 217 | 64 | 0.40 | 5.0 | 7.2 | 189 | 237 |
| | 6.0 | 15 | 0.20 | 10.0 | 7.7 | 140 | 177 | 40 | 0.30 | 6.7 | 7.7 | 151 | 200 | 65 | 0.40 | 5.0 | 7.9 | 171 | 228 |
| 45 | 1.0 | 16 | 0.16 | 12.8 | 7.9 | 283 | 316 | 41 | 0.19 | 10.5 | 12.0 | 310 | 335 | 66 | 0.23 | 8.8 | 8.9 | 315 | 359 |
| | 2.0 | 17 | 0.20 | 10.0 | 7.0 | 174 | 175 | 42 | 0.25 | 8.0 | 9.0 | 240 | 257 | 67 | 0.30 | 6.7 | 12.0 | 297 | 329 |
| | 3.0 | 18 | 0.20 | 10.0 | 9.9 | 149 | 156 | 43 | 0.25 | 8.0 | 9.0 | 200 | 244 | 68 | 0.30 | 6.7 | 8.9 | 245 | 279 |
| | 4.5 | 19 | 0.20 | 10.0 | 8.2 | 142 | 158 | 44 | 0.25 | 8.0 | 8.1 | 162 | 189 | 69 | 0.30 | 6.7 | 7.2 | 158 | 182 |
| | 6.0 | 20 | 0.20 | 10.0 | 8.0 | 139 | 144 | 45 | 0.25 | 8.0 | 8.9 | 172 | 177 | 70 | 0.30 | 6.7 | 11.6 | 156 | 160 |
| 90 | 1.0 | 21 | 0.20 | 10.0 | 10.3 | 322 | 354 | 46 | 0.20 | 10.0 | 8.8 | 321 | 369 | 71 | 0.20 | 10.0 | 7.4 | 306 | 328 |
| | 2.0 | 22 | 0.20 | 10.0 | 9.6 | 180 | 190 | 47 | 0.20 | 10.0 | 12.1 | 199 | 212 | 72 | 0.20 | 10.0 | 7.8 | 208 | 255 |
| | 3.0 | 23 | 0.20 | 10.0 | 9.4 | 155 | 175 | 48 | 0.20 | 10.0 | 8.3 | 170 | 189 | 73 | 0.20 | 10.0 | 7.3 | 178 | 187 |
| | 4.5 | 24 | 0.20 | 10.0 | 7.2 | 138 | 159 | 49 | 0.20 | 10.0 | 6.9 | 151 | 178 | 74 | 0.20 | 10.0 | 7.2 | 143 | 151 |
| | 6.0 | 25 | 0.20 | 10.0 | 7.8 | 121 | 127 | 50 | 0.20 | 10.0 | 7.7 | 135 | 141 | 75 | 0.20 | 10.0 | 7.0 | 140 | 145 |



J. Hydraul. Eng. 2013.139:1089-1098.

Also, with two exceptions (tests 7 and 8), values of $B/W_g < 10$ corresponded to flow shallowness $d/W_g = [0.50; 1.00]$. According to the same authors, for such values of flow shallowness, significant increases of scour depth ascribable to contraction effects may be observed only for $B/W_g < 3$, which is not the case. It is with no surprise that contraction scour was not observed.

It is assumed herein that equilibrium is attained asymptotically. The time records of scour depth were extrapolated to $t = \infty$ through the six-parameter polynomial technique suggested by Lança et al. (2010) as a means to estimate the equilibrium scour depth, $d_{sge}$, associated to each individual pile in the group. The $d_{sge}$ values included in Table 2 are the groups' maxima, irrespective of the location of the pile at which it occurred. The table also registers the deepest scour depths measured at the end of the tests, $d_{sgm}$.

Figs. 2 and 3 present the time records of the scour depths at individual piles directly exposed to the approach flow (piles 1.1, 2.1, 3.1, 4.1 1.2, 1.3; see Fig. 1), for $\alpha = [0°, 30°]$, respectively. Data are organized according to the number of columns of the pile group, $n$, and the normalized pile spacing, $s/D_p$. The longer records were truncated at $t = 200$ h and the scale of the scour depth is the same in both figures to aid comparison. The reference equilibrium scour depth obtained at the single pier with $D_p = 50$ mm, $d_{se1}$, is also plotted (horizontal dashed lines). The complete time records of the scour depth are available at http://w3.ualg.pt/~rlanca/pilegroupsdata.pdf.

### Flow Structure and Scour Mechanisms

At pile groups, the flow structure and its interaction with the mobile bed are rather more complex than at single piers. According to Hannah (1978), depending on the values of $\alpha$ and $s/D_p$, the flow structure may comprise sheltering, interaction of wake vortices, and systems of compressed horseshoe vortices. The flatter bed topography induced by the rear piles may facilitate the mobility of upcoming bed grains, thus reinforcing the scour depth at the upstream piles, as compared with the scour depth at an isolated equal diameter pier. Scour *reinforcement* is quite evident in Fig. 2, particularly for $n = [2, 3]$. This effect tends to attenuate as the pile spacing increases.

Whenever present, *sheltering* leads to the reduction of the approach velocity at downstream piles, weakening the strength of the associated horse-shoe vortices and reducing the scour depth. This was observed in many experiments, but it is not evident in Figs. 2 and 3 since the plotted data refer to piles directly exposed to the approach flow (where the scour depth tends to be maximal).

The vortices from the upstream piles are convected downstream and may interact with the rear piles. In this case, the *interaction of wake vortices* may lead to a downstream increase in sediment entrainment capacity. The scour increase caused by this phenomenon depends on the convection speed of the vortices and the distance between their path and the piles. From Table 2, it can be concluded that, for a given combination of $n$ and $s/D_p$ except $s/D_p = 1$, the scour depth is maximal for $\alpha = 30°$; from Fig. 3, it can also be seen that maximum scour occurs at the rear piles of the first column (piles 3.1 and 4.1, see Fig. 1) when $\alpha = \sim 30°$. This may be interpreted as an indication that such piles are located in the path of the most energetic wake vortices generated upstream.

For the case of piles transverse to the flow, i.e., $\alpha = [0°, 90°]$, the effect of *compression of the inner arms* of the horse-shoe vortices

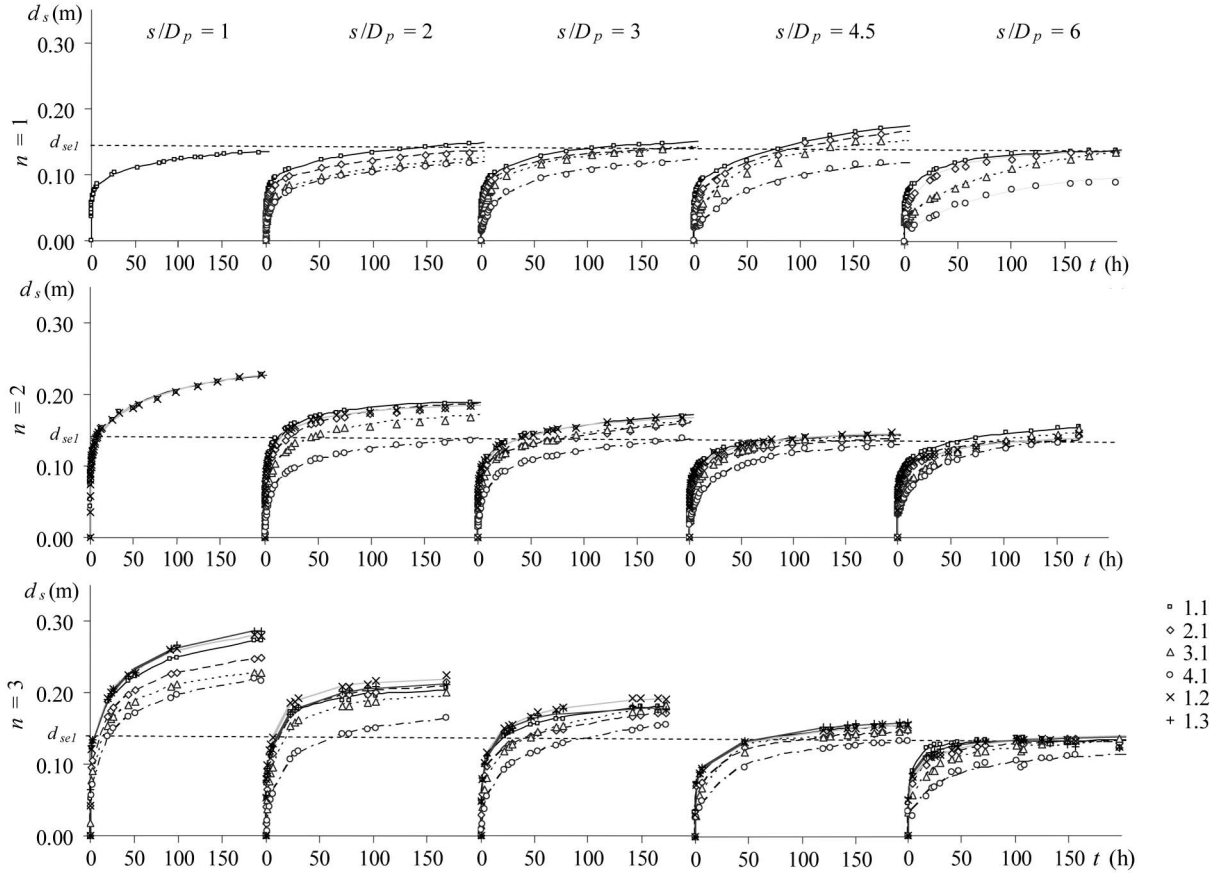


**Fig. 2.** Scour depth time evolution at pile groups for $\alpha = 0°$



J. Hydraul. Eng. 2013.139:1089-1098.

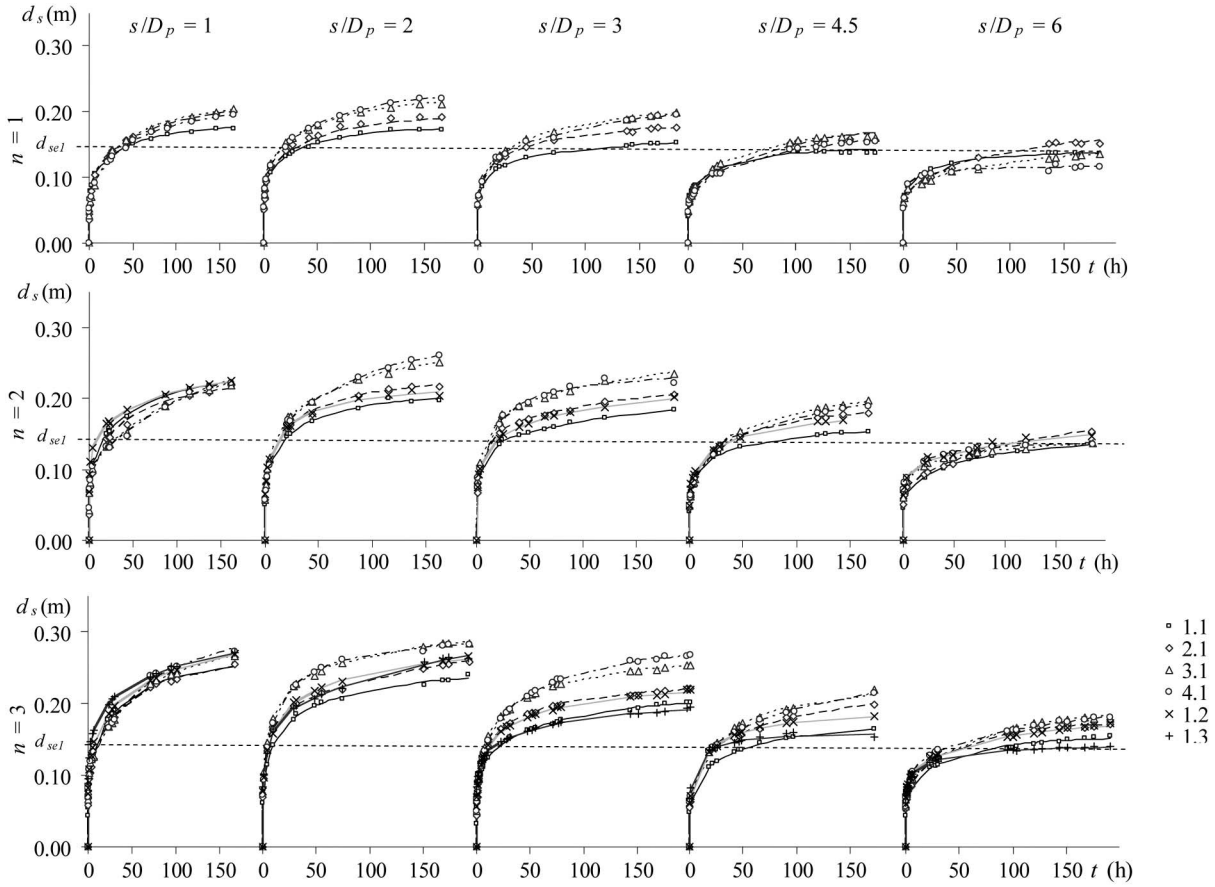


**Fig. 3.** Scour depth time evolution at pile groups for $\alpha = 30°$

can be observed as soon as $s/D_p > 1$. The compressed arms lead to an increase of the local velocity, impacting on the scour depth. This effect increases as the pile spacing decreases. In the limit, for $s/D_p = 1$, the pile group acts as a single pier, with no inner horse-shoe arms. It is important to point out that for $s/D_p \leq 3.0$ a single scour hole was observed. For $s/D_p = 4.5$ the scour holes of the individual piles tend to separate and, for $s/D_p = 6.0$, only weak interaction between scour at each pile was observed. These findings are in agreement with those of Amini et al. (2012).

### *Effect of Time on the Scour Process*

The motivation for the present study derived from the fact that most of the tests reported in the literature so far were carried out for rather short durations. Table 3 summarizes the values of the maxima scour depths measured at $t = [8,24,168]$ hours (168 hours $\equiv$ 7 days) normalized by the equilibrium scour depths, $d_{sge}$. At $t = 8$ hours, the maxima scour depth is only $(0.54 \pm 0.06)$ of the corresponding equilibrium value. The similar statistics for $t = [24,168]$ hours are $(0.65 \pm 0.07)$ and $(0.87 \pm 0.06)$,

**Table 3.** Ratio of Maxima Scour Depths Measured at $t = [8,24,168]$ h and Maxima Equilibrium Scour Depth

| | | $\alpha = 0°$ | | | $\alpha = 15°$ | | | $\alpha = 30°$ | | | $\alpha = 45°$ | | | $\alpha = 90°$ | | |
|---|---|---|---|---|---|---|---|---|---|---|---|---|---|---|---|---|
| | | $T$ (h) | | | $t$ (h) | | | $t$ (h) | | | $t$ (h) | | | $t$ (h) | | |
| $n$ | $s/D_p$ | 8 | 24 | 168 | 8 | 24 | 168 | 8 | 24 | 168 | 8 | 24 | 168 | 8 | 24 | 168 |
| 1 | 1.0 | 0.56 | 0.65 | 0.86 | 0.60 | 0.70 | 0.90 | 0.44 | 0.56 | 0.82 | 0.52 | 0.65 | 0.88 | 0.48 | 0.60 | 0.86 |
| | 2.0 | 0.55 | 0.63 | 0.83 | 0.63 | 0.76 | 0.97 | 0.48 | 0.60 | 0.85 | 0.64 | 0.80 | 0.96 | 0.61 | 0.75 | 0.94 |
| | 3.0 | 0.58 | 0.69 | 0.90 | 0.60 | 0.70 | 0.90 | 0.48 | 0.60 | 0.85 | 0.63 | 0.78 | 0.95 | 0.58 | 0.71 | 0.88 |
| | 4.5 | 0.53 | 0.50 | 0.91 | 0.54 | 0.70 | 0.92 | 0.43 | 0.54 | 0.78 | 0.61 | 0.73 | 0.89 | 0.58 | 0.68 | 0.88 |
| | 6.0 | 0.58 | 0.72 | 0.93 | 0.57 | 0.67 | 0.94 | 0.50 | 0.58 | 0.80 | 0.62 | 0.76 | 0.94 | 0.66 | 0.79 | 0.93 |
| 2 | 1.0 | 0.53 | 0.62 | 0.85 | 0.45 | 0.54 | 0.76 | 0.45 | 0.53 | 0.72 | 0.47 | 0.60 | 0.87 | 0.48 | 0.59 | 0.84 |
| | 2.0 | 0.66 | 0.78 | 0.94 | 0.46 | 0.58 | 0.83 | 0.40 | 0.50 | 0.75 | 0.53 | 0.67 | 0.90 | 0.57 | 0.72 | 0.92 |
| | 3.0 | 0.57 | 0.66 | 0.85 | 0.60 | 0.76 | 0.99 | 0.46 | 0.58 | 0.77 | 0.48 | 0.59 | 0.80 | 0.57 | 0.70 | 0.88 |
| | 4.5 | 0.64 | 0.77 | 0.93 | 0.44 | 0.60 | 0.85 | 0.48 | 0.60 | 0.85 | 0.51 | 0.61 | 0.84 | 0.57 | 0.68 | 0.86 |
| | 6.0 | 0.60 | 0.70 | 0.91 | 0.49 | 0.60 | 0.82 | 0.46 | 0.52 | 0.75 | 0.62 | 0.69 | 0.91 | 0.67 | 0.78 | 0.94 |
| 3 | 1.0 | 0.50 | 0.61 | 0.86 | 0.45 | 0.55 | 0.84 | 0.50 | 0.58 | 0.80 | 0.45 | 0.58 | 0.85 | 0.54 | 0.70 | 0.92 |
| | 2.0 | 0.64 | 0.80 | 0.96 | 0.42 | 0.54 | 0.77 | 0.43 | 0.53 | 0.69 | 0.46 | 0.58 | 0.84 | 0.54 | 0.65 | 0.80 |
| | 3.0 | 0.55 | 0.67 | 0.86 | 0.51 | 0.67 | 0.83 | 0.48 | 0.61 | 0.87 | 0.44 | 0.57 | 0.86 | 0.62 | 0.76 | 0.94 |
| | 4.5 | 0.43 | 0.52 | 0.69 | 0.47 | 0.62 | 0.82 | 0.46 | 0.57 | 0.77 | 0.54 | 0.64 | 0.86 | 0.67 | 0.80 | 1.00 |
| | 6.0 | 0.73 | 0.84 | 0.95 | 0.56 | 0.70 | 0.92 | 0.44 | 0.53 | 0.75 | 0.71 | 0.79 | 0.98 | 0.68 | 0.79 | 0.97 |



J. Hydraul. Eng. 2013.139:1089-1098.

**Table 4.** Values of $\Delta K_{pg}$ at $t = [8,24,168]$ h

| | | $\alpha = 0°$ | | | $\alpha = 15°$ | | | $\alpha = 30°$ | | | $\alpha = 45°$ | | | $\alpha = 90°$ | | |
|---|---|---|---|---|---|---|---|---|---|---|---|---|---|---|---|---|
| | | $t$ (h) | | | $t$ (h) | | | $t$ (h) | | | $t$ (h) | | | $t$ (h) | | |
| $n$ | $s/D_p$ | 8 | 24 | 168 | 8 | 24 | 168 | 8 | 24 | 168 | 8 | 24 | 168 | 8 | 24 | 168 |
| 1 | 1.0 | 0.01 | 0.00 | 0.01 | −0.05 | −0.07 | −0.04 | 0.23 | 0.14 | 0.05 | 0.08 | 0.00 | −0.02 | 0.15 | 0.07 | 0.00 |
| | 2.0 | 0.04 | 0.03 | 0.04 | −0.12 | −0.17 | −0.12 | 0.15 | 0.08 | 0.01 | −0.14 | −0.23 | −0.11 | −0.07 | −0.15 | −0.09 |
| | 3.0 | −0.02 | −0.06 | −0.04 | −0.06 | −0.07 | −0.04 | 0.15 | 0.08 | 0.02 | −0.11 | −0.20 | −0.10 | −0.03 | −0.10 | −0.01 |
| | 4.5 | 0.07 | 0.22 | −0.06 | 0.05 | −0.08 | −0.07 | 0.24 | 0.17 | 0.10 | −0.08 | −0.13 | −0.03 | −0.02 | −0.05 | −0.02 |
| | 6.0 | −0.02 | −0.10 | −0.07 | 0.00 | −0.04 | −0.08 | 0.12 | 0.11 | 0.07 | −0.09 | −0.17 | −0.09 | −0.16 | −0.22 | −0.08 |
| 2 | 1.0 | 0.06 | 0.04 | 0.01 | 0.20 | 0.16 | 0.13 | 0.20 | 0.19 | 0.17 | 0.18 | 0.08 | 0.00 | 0.16 | 0.09 | 0.02 |
| | 2.0 | −0.17 | −0.20 | −0.09 | 0.20 | 0.10 | 0.04 | 0.30 | 0.23 | 0.14 | 0.06 | −0.03 | −0.04 | −0.01 | −0.11 | −0.06 |
| | 3.0 | 0.00 | −0.01 | 0.02 | −0.05 | −0.17 | −0.14 | 0.18 | 0.11 | 0.11 | 0.15 | 0.09 | 0.08 | −0.01 | −0.07 | −0.01 |
| | 4.5 | −0.13 | −0.18 | −0.08 | 0.22 | 0.08 | 0.02 | 0.16 | 0.07 | 0.02 | 0.09 | 0.06 | 0.03 | 0.00 | −0.04 | 0.01 |
| | 6.0 | −0.06 | −0.08 | −0.05 | 0.13 | 0.08 | 0.05 | 0.19 | 0.20 | 0.14 | −0.09 | −0.07 | −0.05 | −0.18 | −0.20 | −0.09 |
| 3 | 1.0 | 0.13 | 0.06 | 0.00 | 0.21 | 0.16 | 0.03 | 0.13 | 0.11 | 0.07 | 0.21 | 0.10 | 0.02 | 0.05 | −0.07 | −0.06 |
| | 2.0 | −0.13 | −0.24 | −0.11 | 0.27 | 0.16 | 0.11 | 0.25 | 0.19 | 0.20 | 0.19 | 0.11 | 0.03 | 0.04 | 0.01 | 0.07 |
| | 3.0 | 0.03 | −0.03 | 0.01 | 0.10 | −0.03 | 0.04 | 0.16 | 0.06 | −0.01 | 0.23 | 0.13 | 0.01 | −0.10 | −0.17 | −0.09 |
| | 4.5 | 0.25 | 0.20 | 0.20 | 0.16 | 0.05 | 0.05 | 0.18 | 0.12 | 0.11 | 0.05 | 0.02 | 0.00 | −0.18 | −0.23 | −0.16 |
| | 6.0 | −0.29 | −0.29 | −0.10 | 0.01 | −0.07 | −0.06 | 0.23 | 0.19 | 0.13 | −0.26 | −0.22 | −0.13 | −0.20 | −0.21 | −0.12 |

respectively, which corroborates the fact that the scour experiments at pile groups lasting less than 7 days may implicitly contain important uncertainties in the equilibrium scour depth.

From Table 3 it becomes clear that, for $\alpha = 30°$, the scour process evolved at a rate that is slower than for the other angles since the corresponding average ratios are [0.46, 0.56, 0.79] for $t = [8,24,168]$ hours, respectively. This reveals that, though the deepest scour holes are observed for $\alpha = 30°$ (*cf.* Table 2), they take a considerable longer time to stabilize than for other configurations.

One specific question investigated in this study is whether the pile group factor, $K_{pg}$, remains unchanged or not as scour evolves in time. The inspection of Table 4 reveals that the values of $\Delta K_{pg}$ given by

$$\Delta K_{pg} = \frac{K_{pge} - K_{pg}}{K_{pge}} \tag{5}$$

where $K_{pg}$ is defined at any time $t$, do not change appreciably in time. Excluding the values corresponding to $\alpha = 30°$, the average absolute values of $\Delta K_{pg}$ are [0.11, 0.11, 0.08] for $t = [8,24,168]$ hours, respectively, while the maximum and the minimum values are 0.27 and −0.29, both for $t = 8$ h. These results indicate that the scour depth at pile groups and at the isolated elemental pier evolve through time at reasonably similar rates, the scour holes remaining essentially self-similar with time. A larger difference is observed for $\alpha = 30°$, where average $\Delta K_{pg} = [0.19, 0.14, 0.09]$ arise for $t = [8,24,168]$ hours, respectively. This means that, despite the short durations of the previous studies and the inherently strong deviations from the equilibrium stage, with marked underevaluation of both $d_{sge}$ and $d_{se1}$, there is no direct experimental reason for coefficients such as the pile spacing coefficient, $K_{sp}$, or the coefficient for the number of aligned rows, $K_m$, integrated in current scour predictors to be unreliable [see, e.g., Richardson and Davis (2001) or Sheppard and Renna (2010)].

### *Dependence of the Pile Group Factor from the Pile Spacing and the Skew Angle*

Table 5 summarizes the values of $K_{pge}$. It should be reiterated here that, in the context of the present study, $K_{pge}$ accounts for several effects, namely, spacing, skew angle and number of columns, $n$. In Fig. 4, the values of $K_{pge}$ are plotted against $\alpha$ and spacing, $s/D_p$, for the three adopted $n$ values.

Referring to $n = 1$ (pier alignment), the joint observation of Fig. 2, Table 5, and Fig. 4(a), shows that for $\alpha = 0°$ the deepest scour hole is always observed at the pier 1.1 (see Fig. 2). The maximum scour depth leads to $K_{pge} \approx 1.15$ (see Table 5) for $s/D_p = [1, 2, 3, 4.5]$, possibly due to the phenomenon of scour reinforcement; the pile group factor decreases to 1.0 for $s/D_p = 6$. For the same case ($n = 1$), $\alpha = 15°$, the values of $K_{pge}$ are not significantly different from those observed for $\alpha = 0°$, conflicting with intuition and some findings reported in the literature (e.g., Zhao and Sheppard 1999). For the other skew angles, $\alpha = [30°, 45°, 90°]$; still, for $n = 1$, scour depth systematically decreases with $s/D_p$. Nevertheless, for $s/D_p = 6$, scour depth shows a weak dependence on $\alpha$; yet $K_{pge}$ values of the order of 1.25 ~ 1.30 were observed for $\alpha = [15°, 30°]$. With the exception of $s/D_p = 1$, the deepest scour holes observed for $n = 1$ occur for $\{\alpha = 30°,\ s/D_p = [2, 3]\}$; in these cases, $K_{pge} \approx 1.7$, while it slightly decreases to 1.3 for $s/D_p = 6$. For $[\alpha = 45°,\ n = 1]$, $K_{pge} \approx 2.3$ as $s/D_p = 1$ and clearly decreases with $s/D_p$, becoming $K_{pge} \approx 1.3$ for $s/D_p = 2$. For $\alpha = 90°$, $n = 1$, and $s/D_p = 1$, the alignment acts as a single pier with one single horse-shoe vortex; the scour depth is the greatest; for $s/D_p = 2$, different horse-shoe vortices are believed to be present, the corresponding arms being compressed by the flow acceleration in the space between the piers. With the increase of $s/D_p$, this group effect tends

**Table 5.** Pile Group Factor, $K_{pge}$

| $n$ | $s/D_p$ | $\alpha = 0°$ | $\alpha = 15°$ | $\alpha = 30°$ | $\alpha = 45°$ | $\alpha = 90°$ |
|---|---|---|---|---|---|---|
| 1 | 1.0 | 1.13 | 1.15 | 1.81 | 2.33 | 2.61 |
| | 2.0 | 1.18 | 1.12 | 1.78 | 1.29 | 1.40 |
| | 3.0 | 1.12 | 1.19 | 1.56 | 1.15 | 1.29 |
| | 4.5 | 1.10 | 1.35 | 1.46 | 1.16 | 1.17 |
| | 6.0 | 1.00 | 1.25 | 1.30 | 1.06 | 0.94 |
| 2 | 1.0 | 1.92 | 2.20 | 2.33 | 2.47 | 2.71 |
| | 2.0 | 1.36 | 1.76 | 2.44 | 1.90 | 1.56 |
| | 3.0 | 1.35 | 1.35 | 2.04 | 1.80 | 1.39 |
| | 4.5 | 1.08 | 1.51 | 1.60 | 1.39 | 1.31 |
| | 6.0 | 1.15 | 1.51 | 1.47 | 1.30 | 1.04 |
| 3 | 1.0 | 2.41 | 2.46 | 2.55 | 2.65 | 2.42 |
| | 2.0 | 1.56 | 2.25 | 2.78 | 2.42 | 1.87 |
| | 3.0 | 1.53 | 1.84 | 2.06 | 2.05 | 1.37 |
| | 4.5 | 1.60 | 1.53 | 1.75 | 1.34 | 1.11 |
| | 6.0 | 1.03 | 1.26 | 1.68 | 1.18 | 1.07 |



J. Hydraul. Eng. 2013.139:1089-1098.

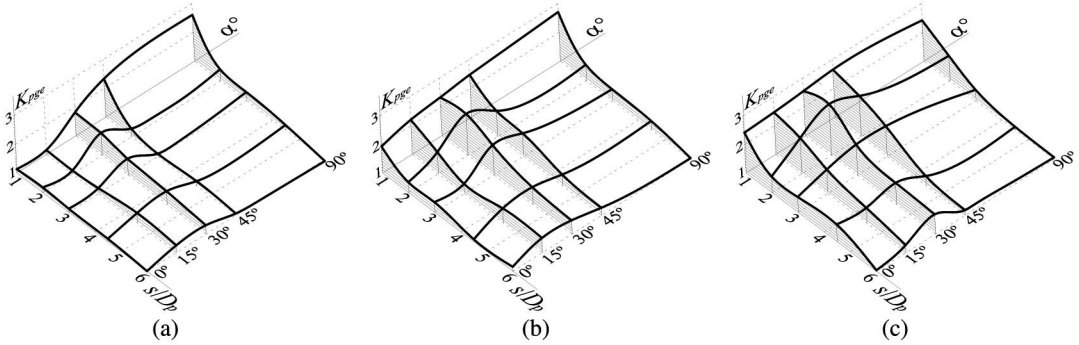


**Fig. 4.** Variation of $K_{pge}$ with $s/D_p$ and $\alpha$ for (a) $n = 1$; (b) $n = 2$; (c) $n = 3$

to vanish and each pier in the alignment $\alpha = 90°$ tends to behave as a single one: the values of $K_{pge}$ for $\alpha = 90°$ are $K_{pge} \approx [2.6, 1.4, 1.3, 1, 0]$ for $s/D_p = [1, 2, 3, 6]$, respectively.

Qualitatively, the overall variation of $K_{pge}$ with $\alpha$ and $s/D_p$ for $n = [2, 3]$ does not significantly differ from the variation described for $n = 1$. However, the analysis of Table 5 and Figs. 4(b and c), shows that, with one single exception [$\alpha = 0°$, $s/D_p = 4.5$], the values of $K_{pge}$ are systematically higher for $n = 2$ than for $n = 1$. This increase is confirmed for $n = 3$ (as compared with $n = 2$) for $s/D_p = [2, 3]$, while a decreasing trend is identified for $s/D_p = 6$ (excluding $\alpha = 30°$). Except for $\{\alpha = 30°, s/D_p = 2, n = [2, 3]\}$, the maximum scour depth is observed for $s/D_p = 1$ as soon as $\alpha > 15°$, irrespective of $n$. The scour depth and the pile group factor $K_{pge}$ significantly increase for small spacing and $\alpha = [0°, 15°]$ as $n$ increases. It can also be remarked that, for $n = 3$, $K_{pge}$ is clearly higher if $\alpha = [0°, 15°]$ and $s/D_p \leq 4.5$ than it is for $n = [1, 2]$.

In view of the experimental evidence described above, the following equation was derived:

$$K_{pge} = \beta \left(\frac{s}{D_p}\right)^{\gamma} n^{\delta}\Big|_{\alpha=\text{const.}} \tag{6}$$

the values of $\beta$, $\gamma$ and $\delta$ being those obtained through regression analysis for each $\alpha$ value. They are included in Table 6, together with the determination coefficient, $r^2$.

Assuming that, instead of $d_{se1}$, the scaling length that best accounts for the scouring process at pile groups is the equilibrium scour depth, $d_{sew}$, at an isolated cylindrical pier of diameter $W_g$, Eq. (4) reads

$$K_{pwe} = \frac{d_{sge}}{d_{sew}} = \varphi\left(\frac{s}{D_p}; \alpha; m; n\right) \tag{7}$$

while Eq. (6) becomes

$$K_{pwe} = \beta_w \left(\frac{s}{D_p}\right)^{\gamma_w} n^{\delta_w}\Big|_{\alpha=\text{const.}} \tag{8}$$

**Table 6.** Coefficients for Different Skew Angles

| angle $\alpha$ | 0° | 15° | 30° | 45° | 90° |
|---|---|---|---|---|---|
| $\beta$ | 1.412 | 1.509 | 1.994 | 2.083 | 2.46 |
| $\gamma$ | −0.295 | −0.234 | −0.234 | −0.407 | −0.538 |
| $\delta$ | 0.389 | 0.425 | 0.292 | 0.284 | 0.041 |
| $r^2$ | 0.81 | 0.77 | 0.81 | 0.9 | 0.94 |
| $\beta_w$ | 1.302 | 0.967 | 1.099 | 1.069 | 1.110 |
| $\gamma_w$ | −0.231 | −0.449 | −0.390 | −0.514 | −0.538 |
| $\delta_w$ | −0.161 | 0.155 | 0.043 | 0.100 | 0.042 |
| $r_w^2$ | 0.67 | 0.85 | 0.96 | 0.91 | 0.94 |

Here, $K_{pwe}$ = pile group factor associated with $W_g$. In this study, it was possible to obtain the empirical values of $d_{sew}$ from the equilibrium scour depth measured at the reference cylindrical piers, $D_p = [50,100,150,200,400]$ mm. The variation of $K_{pwe}$ with $s/D_p$, $\alpha$ and $n$ may be described by an equation structurally similar to Eq. (6); the coefficients $\beta_w$, $\gamma_w$, $\delta_w$ and $r_w^2$ are also included in Table 6.

From the values of the determination coefficients, a slightly improved representation of the scour data through Eq. (8) seems to be achieved as compared with Eq. (6), the only exception corresponding to $\alpha = 0°$. Though based on a large and robust data set, it should be stressed that Eqs. (6) and (8) are strictly limited to the case where $m = 4$.

### Further Discussion

Irrespective of the number of columns in the group, collapsed pile groups defined by $s/D_p = 1$ may be assumed to behave as single rectangular piers with rounded-corners as sketched in Fig. 5 (dashed perimeter). The associated ratios of the equivalent pier length, $L$, to width, $a$, are, $L/a = [4, 2, 4/3]$, for $n = [1, 2, 3]$, respectively, as soon as $\alpha \leq 45°$. For $\alpha = 90°$, $L$ and $a$ may be interchanged, the ratio $L/a$ becoming $L/a = [1/4, 1/2, 3/4]$, which corresponds to assume $m = 3$, $n = 4$ and $\alpha = 0°$ (see Fig. 1).

The idea behind Fig. 5 was first suggested by Salim and Jones (1996). According to these authors, the scour depth at pile groups composed of square piles is equal to the scour depth at single rectangular solid piers whose dimensions are the sum of the dimensions of the individual piles. According to this idea, the following equation may be assumed to hold:

$$d_{sge} = K_\alpha K_s d_{se} \tag{9}$$

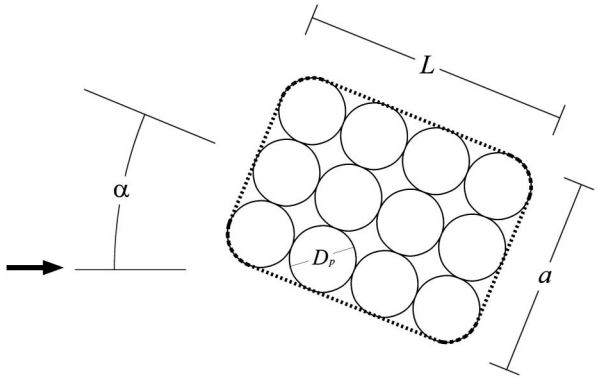


**Fig. 5.** Pile group idealized as a pier for $s/D_p = 1$



J. Hydraul. Eng. 2013.139:1089-1098.

**Table 7.** Shape Coefficients of Idealized Single Piers Defined for $s/D_p = 1$

| $\alpha$ (°) | $a$ (m) | $L$ (m) | $K_s$ |
|---|---|---|---|
| 0 | 0.050 | 0.200 | 1.13 |
| 0 | 0.100 | 0.200 | 1.20 |
| 0 | 0.150 | 0.200 | 1.30 |
| 90 | 0.200 | 0.050 | 1.19 |
| 90 | 0.200 | 0.100 | 1.24 |
| 90 | 0.200 | 0.150 | 1.10 |

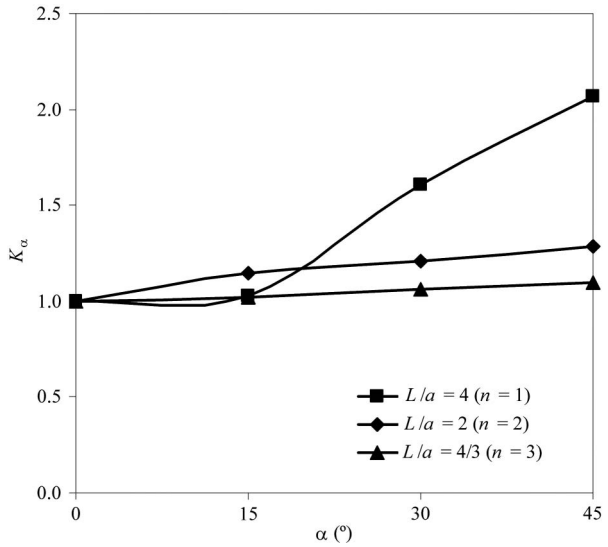


**Fig. 6.** Variation of angle factor, $K_\alpha$, with $\alpha$ and $n$

where $K_\alpha$ = skew-angle coefficient, $K_s$ = shape coefficient of the idealized pier and $d_{se}$ = equilibrium scour depth at the reference cylindrical pier defined by $D_p = a$, for $\alpha = 0°$ and $D_p = L$ for $\alpha = 90°$.

For $n = [1, 2, 3]$ and $\alpha \leq 45°$, pier dimensions are $L = 0.20$ m and $a = [0.050, 0.100, 0.150]$ m, respectively; for $\alpha = 90°$, $a = 0.200$ m and $L = [0.05, 0.100, 0.150]$ as $n = [1, 2, 3]$. The equilibrium scour depth measured at the reference cylindrical piers, $D_p = [50,100,150,200]$ mm was $d_{se} = [0.136, 0.218, 0.252, 0.297]$ m, leading to $d_{se}/D_p = [2.72, 2.18, 1.68, 1.48]$. These values of the normalized scour depth compare with [2.40, 2.40, 2.31, 2.00] calculated through the predictor of Melville and Coleman (2000). The value of $d_{se}/D_p = 2.72$ observed for $D_p = 50$ mm exceeds 2.4, which is possibly imputable to the long duration of the present tests as well as to the improved assessment of the equilibrium scour depth resulting from the extrapolation of the scour records to $t = \infty$. The lower values of $d_{se}/D_p$ observed for $D_p = [100,150,200]$ mm are due to the fact that $D_p/D_{50} = [116,175,232]$ exceed $50 \sim 100$, while the effect of $D_p/D_{50}$ is not accounted for by Melville and Coleman (2000).

The ratios of the equilibrium scour depth at pile groups defined by $s/D_p = 1$ and $\alpha = [0°, 90°]$ to those of isolated equal-width piers led to the $K_s$ values included in Table 7. They are of the same order of magnitude as those suggested, for instance, by Melville and Coleman (2000) ($K_s = 1.1$), though slightly higher. This small increase is ascribable to the lateral recesses of the collapsed pier that influence the detachment of erosive wake vortices.

The $K_\alpha$ values plotted against $\alpha$ for each $n$ in Fig. 6 where obtained by dividing the equilibrium scour depth at the pile groups defined by $\alpha \neq [0°, 90°]$ by the values of $K_s$ included in Table 7, and then by the values of $d_{se}$ at the equal width cylindrical pier. Fig. 6 shows that $K_\alpha$ depends on the number of columns, $n$, i.e, on the ratio $L/a$. For $\alpha > 15°$, $K_\alpha$ decreases as $n$ increases, reflecting the tendency for the pile group to approach the cylindrical shape, this way becoming less dependent on the orientation relative to the flow direction.

Compared with the values of $K_\alpha$ suggested by, e.g., Melville and Coleman (2000) or Richardson and Davis (2001) for solid rectangular piers, those plotted in Fig. 6 are slightly smaller for $L/a = 4$, particularly for $\alpha = 15°$, but they are practically the same for $L/a = 2$. The deviations are within common experimental scatter.

In view of the quality of the present data set, the applicability of two current engineering methods used to calculate the scour depth at pile groups–those of Richardson and Davis (2001) and Sheppard and Renna (2010)–was assessed. Their predictions are compared with the measurements in Fig. 7. The most important conclusion is that both methods may underestimate the scour depth. The predictions of Sheppard and Renna (2010) are scattered around the line

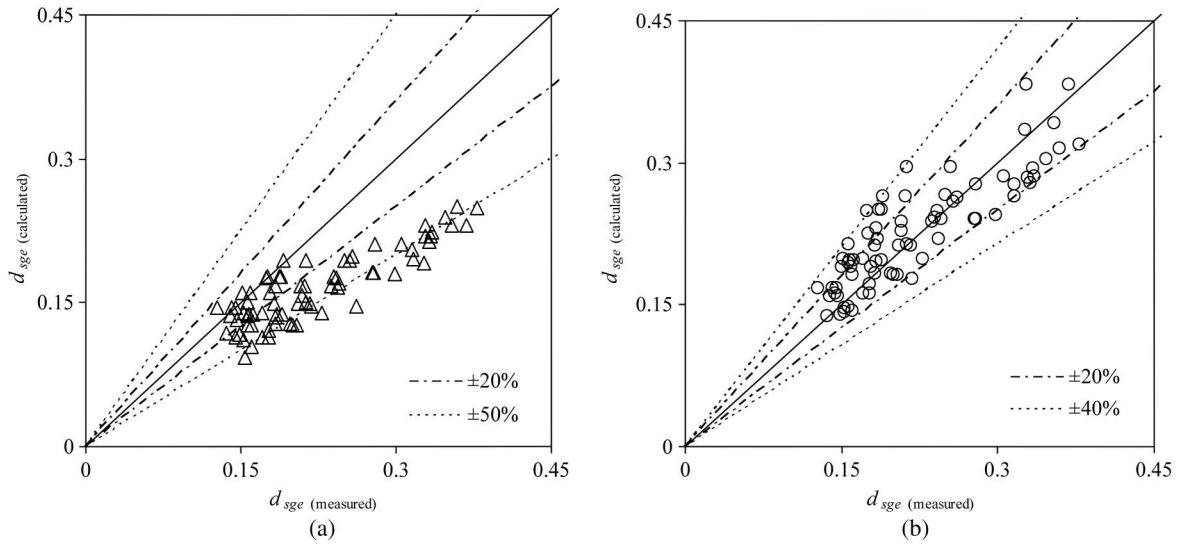


**Fig. 7.** Measured versus calculated scour depths: (a) through the method of Richardson and Davis (2001); (b) through the method of Sheppard and Renna (2010)



J. Hydraul. Eng. 2013.139:1089-1098.

of perfect agreement within a band defined by −20% and +40%. Increasing the scour predictions by a factor of 1.2 seems enough to reproduce the lower bound of the scour depths measured in this study.

On the contrary, the predictions of Richardson and Davis (2001) almost systematically underestimate the scour depth; in many cases, the underestimation is more than 50%. The possible sources for this discrepancy are discussed next. For partly submerged pile groups built of cylindrical piles inserted in uniform sand in the absence of bed-forms, the predictor of Richardson and Davis (2001) reads

$$\frac{d_{sge}}{d} = 2 \times 1.1 \left(\frac{D_{pg}}{d}\right)^{0.65} \mathsf{F}^{0.43} \tag{10}$$

where $D_{pg}$ = effective diameter of the equivalent solid pier; and $\mathsf{F} = U/(gd)^{0.5}$ = approach flow Froude number. According to Richardson and Davis (2001), the effective diameter, $D_{pg}$, is in turn given by

$$D_{pg} = K_{sp} K_m W_g \tag{11}$$

with $K_{sp}$ = coefficient for pile spacing and $K_m$ = coefficient for the number of aligned rows. Those authors offer predictors for $K_{sp}$ and $K_m$.

The inversion of Eq. (10) allowed a back calculation of the values of $D_{pg}$ corresponding to the observed $d_{sge}$. For $\alpha = 0°$ and $n = 1$, the method predicts $K_{sp} = 1$ and $D_{pg}$ becomes $D_{pg} = K_m D_p$ (since $W_g = D_p$). The values of $K_m$ back calculated from tests 1–6 using this method are 1.44–2.51 times those directly calculated through the predictor suggested by Richardson and Davis (2001). From the entire data set, it was also concluded that the ratio between the product $K_{sp}K_m$ back calculated from the measured scour depths is $1.85 \pm 0.42$ times those directly calculated through the predictors; this ratio varies between 1.04 and 2.85. This fact raises the question whether the discrepancies are the result of inappropriate predictors of $K_{sp}$ and $K_m$ or the result of an imprecise scour predictor itself [Eq. (10)] or both. The application of Eq. (10) to the prediction of maximum scour depth at the five single cylindrical piers tested in the present work, produced $d_{se} = [0.093, 0.147, 0.191, 0.230, 0.361]$ m for $D_p = [50, 100, 150, 200, 400]$ mm, respectively, while the observed scour values where [0.136, 0.218, 0.252, 0.297, 0.402] m, i.e., [1.46, 1.48, 1.32, 1.29, 1.11] times deeper. These values show that, on top of the discrepancies due to $K_m$, part of the underprediction is ascribable to the basic scour equation while there is no direct evidence on the performance of the predictor $K_{sp}$. Yet, since this is the same in both assessed methods and the method of Sheppard and Renna (2010) reasonably reproduces the measurements, this may be interpreted as an indication that $K_{sp}$ is properly predicted.

## Conclusions

The present study focus on the effect of pile spacing, skew angle and number of columns of the pile group on the maximum scour depth at pile groups composed of cylindrical piles inserted in uniform, fully-developed turbulent flows in wide rectangular channels with flat bed composed of uniform, non-ripple forming sand. The effect of time on scouring at pile groups is also investigated. It was shown that scour experiments at pile groups lasting less than 7 days may implicitly contain important uncertainties on the equilibrium scour depth. However, in spite of the short durations of the previous studies and the inherent deviations from equilibrium scour, it would seem that coefficients such as the pile spacing coefficient or the coefficient for the number of aligned rows may be reliable, since the scour depth at pile groups remains essentially self-similar in time.

With the exception of $s/D_p = 1$ (collapsed pile group), the maximum scour depth occurs for $\alpha = 30°$. For this configuration ($\alpha = 30°$), the maxima scour depths tend to occur at the rear piles of the first column, which may be interpreted as an indication that such piles are located in the path of the most energetic wake vortices generated upstream. Collapsed pile groups tend to behave as single piers whose dimensions are the sum of the dimensions of the individual piles, reiterating the suggestion of Salim and Jones (1996). Pier alignments, defined by $n = 1$, tend to behave as single piers for $s/D_p \geq 6$, except for $\alpha = [15°, 30°]$, where scour reinforcement is observed.

Safe predictions of the pile group factor, defined as the ratio between the maximum scour depth at a pile group and the maximum scour depth at an isolated elemental cylindrical pier under the same hydrodynamic conditions, can be obtained using Eq. (6), which may be useful in practice if a precise predictor of scour at an isolated single pier is applied. Eq. (8) constitutes an alternative to Eq. (6), in which case the scaling depth is the equilibrium scour depth at a cylindrical pier whose diameter is $W_g$, i.e., the sum of the nonoverlapping pier-widths projected in a plane normal to the approach flow.

The methods of Richardson and Davis (2001) and Sheppard and Renna (2010) may both underpredict the scour depth at pile groups. However, a multiplying factor of $\approx$1.2 applied to the predictions of Sheppard and Renna (2010) seems enough to reproduce the lower bound of measured scour depths. The deviations of the method of Richardson and Davis (2001) seem to be induced by the predictor of scour depth at single piers as well as by the predictor of the coefficient for the number of aligned rows, $K_m$.

## Acknowledgments

The authors wish to acknowledge the financial support of the Portuguese Foundation for Science and Technology trough the research project PTDC/ECM/101353/2008.

## Notation

*The following symbols are used in this paper:*

$a$ = pier width;
$B$ = channel width;
$D_p$ = pile width or diameter;
$D_{pg}$ = equivalent solid pier diameter;
$D_{50}$ = median sediment size;
$d$ = approach flow depth;
$d_{se}$ = equilibrium scour depth at the reference cylindrical pier;
$d_{sew}$ = equilibrium scour depth at an isolated cylindrical pier of diameter $W_g$;
$d_{se1}$ = equilibrium scour depth at an isolated elemental pier or pile;
$d_{sg}$ = pile group scour depth at instant $t$;
$d_{sge}$ = pile group equilibrium scour depth;
$d_{sm}$ = measured scour depth at the end of the test;
$\mathsf{F}$ = Froude number;
$g$ = gravitational acceleration;
$K_m$ = coefficient for the number of aligned rows;
$K_{pg}$ = pile group factor at a given time $t$;
$K_{pge}$ = pile group factor at $t = \infty$;
$K_{pwe}$ = pile group factor associated with $W_g$;



J. Hydraul. Eng. 2013.139:1089-1098.

$L$ = equivalent pier length;
$K_s$ = pier shape factor;
$K_{sp}$ = pile group spacing factor;
$K_\alpha$ = skew-angle factor;
$m$ = number of piles in the alignment; number of group rows;
$n$ = number of pile columns in the group;
$s$ = pile spacing;
$t$ = time;
$t_d$ = test duration;
$U$ = average approach flow velocity;
$U_c$ = average approach flow velocity for the threshold condition of sediment entrainment;
$W_g$ = sum of the nonoverlapping individual pile widths projected on a plane normal to the approach flow;
$\alpha$ = pile group skew-angle;
$\beta$, $\gamma$, and $\delta$ = constants;
$\Delta K_{pg}$ = deviation of the pile group factor with $t$;
$\varphi$ = generic function;
$\rho_s$ = sediment density; and
$\sigma_D$ = sediment gradation coefficient.

## References


Amini, A., Melville, B. W., Ali, T. M., and Ghazali, A. H. (2012). "Clear-water local scour around pile groups in shallow-water flow." *J. Hydraul Eng.*, 138(2), 177–185.

Ataie-Ashtiani, B., and Beheshti, A. A. (2006). "Experimental investigation of clear-water local scour at pile groups." *J. Hydraul Eng.*, 132(10), 1100–1104.

Ballio, F., Teruzzi, A., and Radice, A. (2009). "Constriction effects in clear-water scour at abutments." *J. Hydraul Eng.*, 135(2), 140–145.

Elliott, K. R., and Baker, C. J. (1985). "Effect of pier spacing on scour around bridge piers." *J. Hydraul Eng.*, 111(7), 1105–1109.

Hannah, C. R. (1978). "Scour at pile groups." *Report No. 78–3*, M.S. thesis, Canterbury Univ., Canterbury, New Zealand.

Lança, R., Fael, C., and Cardoso, A. (2010). "Assessing equilibrium clear-water scour around single cylindrical piers." *Proc., River Flow 2010*, A. Dittrich, et al., eds., Bundesanstalt für Wasserbau, Germany, 1207–1213.

Lança, R., Fael, C., Maia, R., Pêgo, J., and Cardoso, A. (2012). "Effect of spacing and skew-angle on clear-water scour at pier alignments." *Proc., RiverFlow 2012*, R. Muñoz, ed., CRC Press, Boca Raton, FL, 927–933.

Melville, B. W., and Coleman, S. E. (2000). *Bridge scour*, Highlands Ranch Water Resources, Highlands Ranch, CO.

Neil, C. R. (1967). "Mean velocity criterion for scour of coarse uniform bed-material." *Proc., 12th IAHR Congress*, IAHR, Fort Collins, CO, 46–54.

Richardson, E. V., and Davis, S. R. (2001). "Evaluating scour at bridges." *Hydraulic Engineering Circular No. 18 (HEC-18), Rep. No. FHWA NHI 01-001*, Federal Highway Administration, Washington, DC.

Salim, M., and Jones, J. S. (1996). "Scour around exposed pile foundations." *Proc., North American Water and Environment Conference '96*, ASCE, Anaheim, CA.

Sheppard, D. M., and Renna, R. (2010). *Bridge scour manual*, Florida Department of Transportation, Tallahassee, FL.

Simarro, G., Fael, C. M. S., and Cardoso, A. H. (2011). "Estimating equilibrium scour depth at cylindrical piers in experimental studies." *J. Hydraul Eng.*, 137(9), 1089–1093.

Smith, W. L. (1999). "Local structure-induced sediment scour at pile groups." M.S. thesis, Univ. of Florida, Gainesville, FL.

Sumer, B. M., and Fredsøe, J. (2002). "The mechanics of scour in the marine environment." *Advanced series on ocean engineering*, World Scientific Publishing, Singapore.

Zhao, G., and Sheppard, D. M. (1999). "The effect of flow skew angle on sediment scour near pile groups." *Stream Stability and Scour at Highway Bridges, Compilation of Conference Papers*, ASCE, Reston, VA, 377–391.






J. Hydraul. Eng. 2013.139:1089-1098.